Review

Binding of carbohydrates and protein inhibitors to the surface of α-amylases

Sophie Bozonnet[1,2], Birgit C. Bønsager[1,2], Birte Kramhøft[1,2], Haruhide Mori[2,3], Maher Abou Hachem[1], Martin Willemoës[1,2], Morten T. Jensen[2], Kenji Fukuda[1,2], Peter K. Nielsen[2,4], Nathalie Juge[5], Nushin Aghajari[6], Samuel Tranier[6], Xavier Robert[6], Richard Haser[6] & Birte Svensson[1,2]*

[1] *Biochemistry and Nutrition Group, BioCentrum-DTU, Technical University of Denmark, Søltofts Plads, Bldg. 224, DK-2800 Kgs. Lyngby, Denmark; phone: ++ 45 4525 2740, fax: ++ 45 4588 6307, e-mail: bis@biocentrum.dtu.dk*
[2] *Department of Chemistry, Carlsberg Laboratory, Gamle Carlsberg Vej 10, DK-2500 Copenhagen Valby, Denmark*
[3] *Permanent address: Division of Applied Bioscience, Graduate School of Agriculture, Hokkaido University, Sapporo 060-8589, Japan*
[4] *Permanent address: Insulin Engineering, Department of Preformulation and Analysis, Novo Nordisk A/S, DK-2880 Bagsvaerd, Denmark*
[5] *Institute of Food Research, Norwich Research Park, Colney, Norwich NR4 7UA, UK*
[6] *Laboratorie de BioCristallographie, Institut de Biologie et Chimie des Protéines, UMR 5086-CNRS/UCBL1, IFR128 "Bio-Sciences, Lyon-Gerland", F-69367, Lyon, France*

Abstract: This review on barley α-amylases 1 (AMY1) and 2 (AMY2) addresses rational mutations at distal subsites to the catalytic site, polysaccharide hydrolysis, and interactions with proteinaceous inhibitors. Subsite mapping of barley α-amylases revealed 6 glycone and 4 aglycone substrate subsites. Moreover, two maltooligosaccharide surface binding sites have been identified. Engineering of outer subsites -6 and $+4$ alters action patterns and relative specificities. Thus, compared to wild-type, Y105A AMY1 (subsite -6) shows 140%, 15%, and <1% and T212Y (subsite $+4$) 32%, 370%, and 90% activity towards starch, maltodextrin, and maltoheptaoside, respectively. The enzyme kinetic properties and modeled maltododecaose complexes suggest binding mode multiplicity. Following an initial hydrolytic cleavage of amylose, an average of 1.9 bonds are cleaved per enzyme-substrate encounter, defining a degree of multiple attack (DMA) of 1.9. DMA increased to 3.3 for Y105A and decreased to 1–1.7 for other subsite mutants. The fusion of a starch-binding domain to AMY1 raised the DMA to 3.0 and increased the amount of higher oligosaccharide products. Remarkably, the subsite mutants had unchanged distribution of released oligosaccharides of DP 5–9, but the profiles differed for the shorter products. A recently identified surface binding site, found exclusively in AMY1, involves the conserved Tyr^{380} which has no effect on the DMA, but proved critical for β-cyclodextrin binding as shown by mutational and surface plasmon resonance analyses. Accordingly, AMY2 has lower affinity for β-cyclodextrin. Hydrolysis of amylopectin proceeds via a fast and a slow reaction rate, with β-cyclodextrin inhibiting the fast one, implicating a distinct role for Tyr^{380} in activity on amylopectin. Barley seeds produce different proteinaceous inhibitors acting specifically on insect, animal or plant α-amylases. Rational mutagenesis of barley α-amylase/subtilisin inhibitor (BASI) identified structural elements responsible for AMY2 inhibition and demonstrated the importance of ionic bonds for inhibitory activity.

Key words: barley α-amylase, subsite mutants, isozyme chimeras, secondary binding sites, degree of multiple attack, amylopectin, proteinaceous inhibitors.

Abbreviations: AMY1, barley α-amylase isozyme 1; AMY2, barley α-amylase isozyme 2; BASI, barley α-amylase/subtilisin inhibitor; BMAI, barley monomeric α-amylase inhibitor; BDAI, barley dimeric α-amylase inhibitor; DMA, degree of multiple attack; GH, glycoside hydrolase family; SBD, starch-binding domain; SPR, surface plasmon resonance; Trx-h, thioredoxin h.

Introduction

Starch-degrading enzymes accommodate substrates at an array of binding subsites that extends from the catalytic site. Substrate can also be bound elsewhere on the enzyme surface, and the binding area may be expanded by auxiliary specific carbohydrate binding modules (Sorimachi et al., 1997; Coutinho & Henrissat,

* Corresponding author

1999; Giardina et al., 2001; Robert et al., 2003). The majority of starch-hydrolases belong to glycoside hydrolase family 13 (GH13) that contains also transferases and isomerases (http://afmb.cnrs-mrs.fr/CAZY; MacGregor et al., 2001). GH13 and the related GH70 and GH77 constitute GH clan H and share a characteristic catalytic $(\beta/\alpha)_8$-barrel domain, which is circularly permuted in GH70 (MacGregor et al., 1996). α-Amylases hydrolyse α-1,4 glucosidic bonds in an endo-fashion. Other endo-acting GH13 members, i.e., isoamylase, pullulanase, and neopullulanase, hydrolyse α-1,6 bonds. The three invariant catalytic residues in GH-H are located near the C-terminus of β-strands 4, 5, and 7, and the broad diversity of enzyme specificities stems from variation in the substrate binding site created by $\beta \rightarrow \alpha$ connecting segments (MacGregor et al., 2001).

Structures of barley α-amylase 1 (AMY1) and 2 (AMY2) in complex with oligosaccharides or protein inhibitors (Kadziola et al., 1998; Vallée et al., 1998; André et al., 1999; Robert et al., 2002a, b, 2003) have facilitated structure/function relationship investigations by mutational analysis of: (i) the impact of outer regions of the binding site on substrate specificity (Bak-Jensen et al., 2004); (ii) the mechanism of multiple attack (Kramhøft et al., 2005); and (iii) the function of a secondary binding site located in the C-terminal domain (Robert et al., 2003). Various structural features are proposed to: (i) discriminate interaction with amylose and amylopectin (Willemoës, M., Bozonnet, S., Kramhøft, B. & Svensson, B, in preparation); (ii) assist in granular starch degradation (Juge et al., 2002); and (iii) recognise proteinaceous inhibitors (Svensson et al., 2004; Bønsager et al., 2005).

Impact of outer subsites on specificity

Six single and two double AMY1 mutants were designed to explore subsites −6 and +4 (Bak-Jensen et al., 2004). Previous mutations at subsite −1 of Asp^{180}, Glu^{205}, and Asp^{291} and two conserved histidines, His^{93} and His^{290} (Søgaard et al., 1993), from GH13 sequence motifs at $\beta \rightarrow \alpha$ loops 3, 4, 5, and 7 (MacGregor et al., 2001), proved these residues to be essential for catalysis and transition-state stabilization. Considerably higher activity on selected substrates and shifted subsite occupancy of oligosaccharides was obtained for mutants at inner aglycone- or glycone-binding subsites +1/+2 (Matsui & Svensson, 1997; Mori et al., 2001) and −2/−3 (Mori et al., 2002). This could also be achieved by engineering of outer glycone-binding subsite −5 (Mori et al., 2001), and a second shell interaction associated with hydrophobic clusters adjacent to the catalytic site (Gottschalk et al., 2001). These findings attest the considerable potential of subsite engineering as a tool to improve activity, although rational design is not always straightforward.

Only a few structural models of amylolytic enzymes have substrate analogues accommodated at the entire binding crevice (Brzozowski et al., 2000). The investigation of remote binding subsites −6 and +4 at the ends of the cleft in AMY1 provided insight into features related to action on polysaccharides (Bak-Jensen et al., 2004). Recently, the inactive catalytic nucleophile mutant AMY1 D180A in complex with maltoheptaose highlighted interactions at subsites −1 through −7 (Robert et al., 2005). Structural data on aglycone contacts, however, are limited to subsites +1 and +2 (Kadziola et al., 1998; Robert et al., 2005). Engineering to Y105A/F/W at Tyr^{105} (AMY1 numbering), stacking onto the glucosyl moiety at subsite −6 in AMY1 and AMY2 (André & Tran, 1999), was guided by modeled maltododecaose complexes (Fig. 1; Bak-Jensen et al., 2004). This elimination and the possible introduction of aromatic stacking in T212Y/W (subsite +4) were combined in Y105A-T212W/Y AMY1. While Y105A displayed drastically reduced activity towards oligosaccharides, it surprisingly showed increased activity on starch (Table 1). By contrast, T212Y/W improved activity on amylose DP17 due to increased affinity, but lost 50% activity on starch. These findings suggest that wild-type Tyr^{105} hampered action on starch. Starch therefore is tentatively proposed to prefer the S1 binding mode over the energetically more favorable S2 maltododecaose (Fig. 1; Bak-Jensen et al., 2004). Secondly, T212W/Y mutants favored maltodextrin over starch, perhaps directing maltodextrin to adopt the S3 binding mode aided by aromatic contacts created at subsites +3/+4. The influence of Y105A dominated in the double mutants that lost the improved affinity for amylose DP17 achieved for T212Y/W AMY1. T212Y mimics AMY2 Tyr^{211}, but AMY2 has higher K_m than AMY1 and the improvement apparently stems from favorable combination of interactions existing in AMY1 and achieved by the mutation.

Subsites −6/+4 double mutants Y105A-T212W/Y reduced activity on amylose DP17 more than the single mutants as shown by the low k_{cat}/K_m values (Table 1). Thus the conformation of the substrate chain and productive binding along the entire length of the binding cleft seem to be optimized in the wild-type enzyme, and is impeded by simultaneous modification of subsites −6 and +4. It appears that degradation of maltodextrin, as opposed to starch, benefited from stacking at subsite −6, i.e., adopting the S2 binding mode (Fig. 1).

Bond cleavage patterns of 4-nitrophenyl maltooligosaccharides changed for subsite mutants. Elimination and introduction of an aromatic group at subsites −6 and +4 cooperated to result in additional substrate interactions at aglycone binding subsites (Bak-Jensen et al., 2004). The high-affinity subsite −6 clearly suppressed shifting of the maltoheptaoside-binding position, whereas the two shorter substrates DP5 and DP6 moved in both T212Y/W and the double mutants to cover subsites +3/+4.

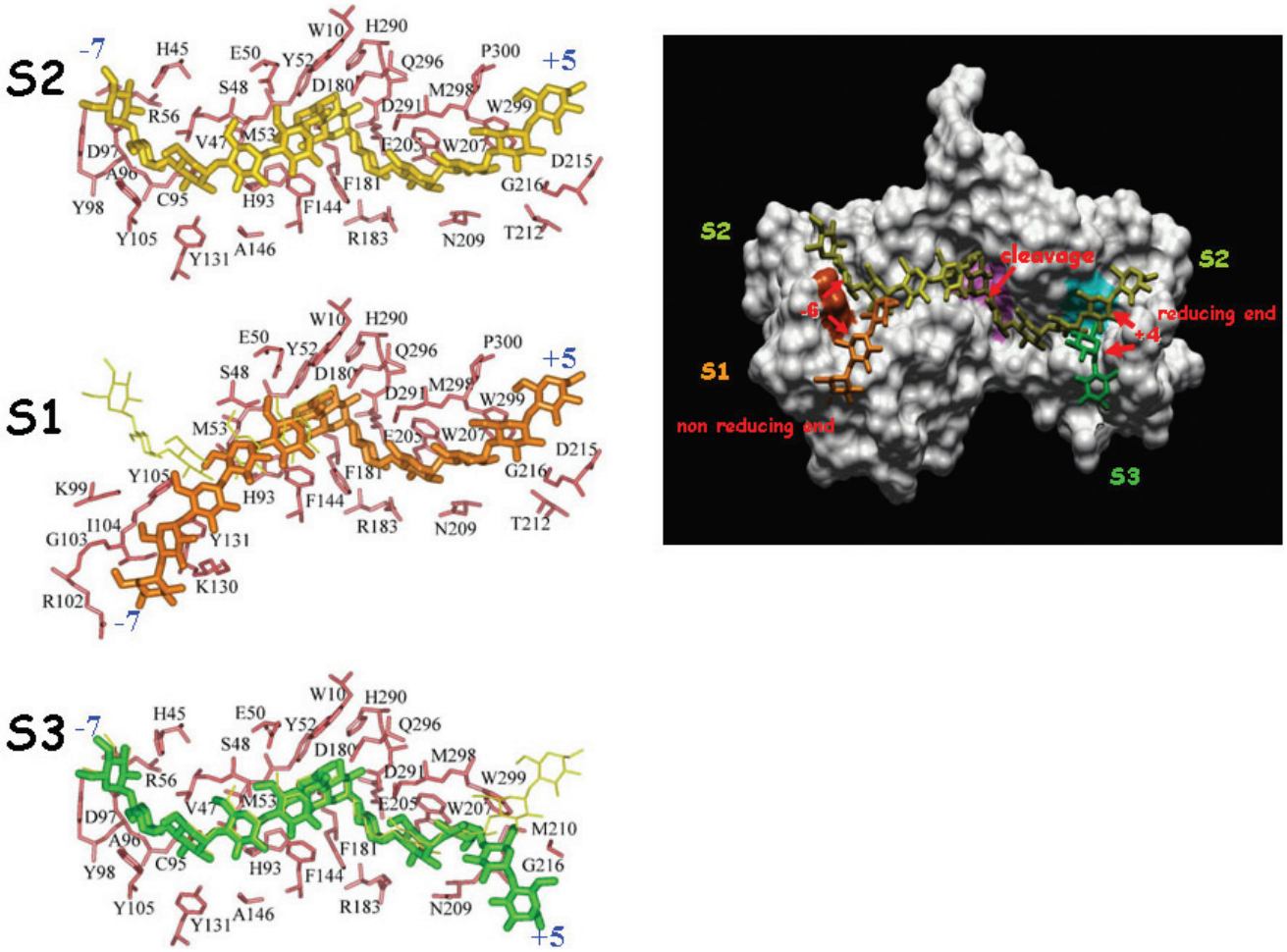

Fig. 1. Modeling of maltododecaose binding in three different modes to barley α-amylase 1 and superimposition in the substrate binding area. Adapted with permission from Bak-Jensen et al. (2004).

Table 1. Enzymatic activities of subsite −6 and +4 mutants of barley α-amylase 1.

AMY1[a]	Cl-pNPG$_7$			Amylose DP17			Insoluble blue starch
	k_{cat} s^{-1}	K_m mM	k_{cat}/K_m s^{-1} mM^{-1}	k_{cat} s^{-1}	K_m mg mL^{-1}	k_{cat}/K_m s^{-1} mg^{-1} mL	U mg^{-1}
Y105A	<10	>10	–	146	2.4	62	3400
Y105F	203	4.9	41	158	0.58	272	2800
T212W	61	0.6	102	154	0.29	531	1400
T212Y	127	2.0	64	127	0.12	1058	1200
Y105A-T212W	24	3.1	8	105	2.0	53	2500
Y105A-T212Y	31	6.0	5	78	2.3	34	1800
Wild-type	119	1.7	70	165	0.57	289	2500

[a] From Bak-Jensen et al. (2004).

Hence, it can be postulated that aromatic stacking of glycosyl moieties at the ends of the binding cleft impeded degradation of polysaccharides by AMY1 wild-type and T212Y/W, but that such interactions promoted hydrolysis of oligosaccharides and short maltodextrins presumably due to increased overall affinity for these substrates.

An important outcome of the outer subsite mutations was the change of the relative substrate preference. For instance, Y105A compared to wild-type AMY1 favored degradation of starch over oligosaccharide and maltodextrin by 100 and 6 fold, respectively, which is also observed as an increased activity for starch. Moreover, T212Y raised activity on maltodextrin to 350% of AMY1 wild-type and essentially maintained activity for a maltoheptaoside, while showing modestly reduced activity for starch (Bak-Jensen et al., 2004).

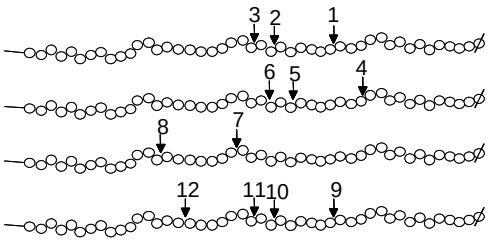

Fig. 2. Schematics of multiple attack reaction. Substrate binds to enzyme, which cleaves the first glucosidic bond (at 1), and subsequently slides to perform new attacks at 2 and 3 before dissociation. A new primary attack occurs at 4, etc.

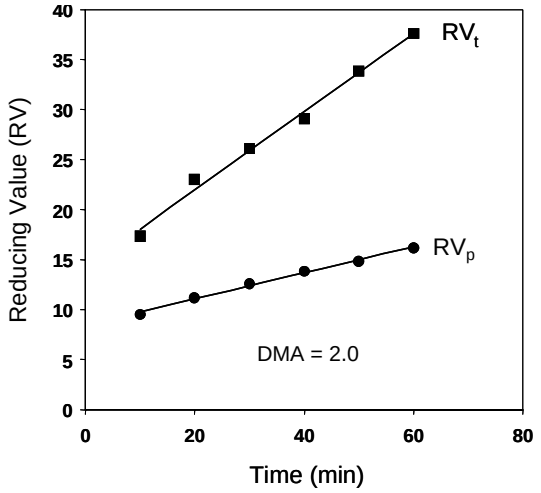

Fig. 3. Determination of degree of multiple attack (DMA). Reducing values of a total digest of amylose and in the corresponding polysaccharide fraction obtained after ethanol precipitation were measured, using maltose as the standard, and the rates of reducing power formation (RV_t and RV_p) were calculated by linear regression. DMA is obtained using the relationship: DMA = $(RV_t/RV_p) - 1$.

Degradation of polysaccharides

α-Amylases can hydrolyse amylose according to a multiple attack mode in which the degree of multiple attack (DMA), defined as the number of substrate bonds hydrolyzed subsequent to the initial cleavage but prior to dissociation of the enzyme-substrate complex, is variable (Robyt & French, 1967; Kramhøft et al., 2005). Amylose DP440, used in the present work, is believed to be hydrolyzed initially in an endo-action yielding two high-molecular mass products. The glycone-moiety is proposed to remain bound to the enzyme and undergoes additional bond cleavages near the reducing end resulting in the release of shorter products (Fig. 2). The ratio of the rates of formation of oligomer and polymer molecules determines the DMA (Kramhøft et al., 2005). This involves analyses of the reducing power of ethanol-soluble and ethanol-insoluble fractions in aliquots removed from the reaction mixture during the initial stage of hydrolysis (Fig. 3).

Mutations at a specific subsite are likely to influence the affinity of that subsite, and thus the positioning of substrate in the binding cleft which ultimately might affect the DMA. DMA was 1.9 for AMY1 wild-type and 1.0-3.3 for different subsite mutants. Maltoheptaose was in all cases the predominant product and maltose, maltohexaose, and DP 8-10 maltooligosaccharides were also major products. Most remarkably, the mutations did not change the distribution of released products of DP 5-10, while the shorter products varied enormously (Fig. 4).

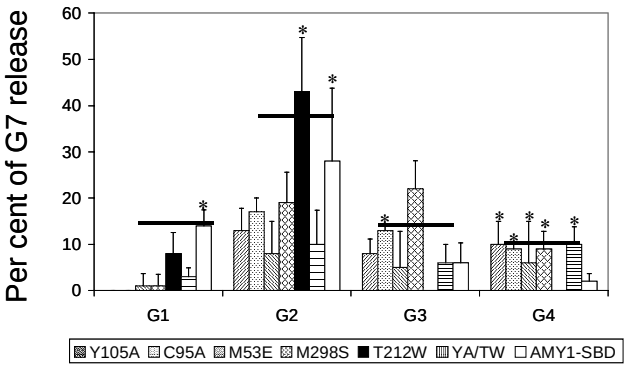

Fig. 4. Oligosaccharide products DP 1-4 of amylose DP440 hydrolysis by AMY1 variants. The rates of appearance of each product were normalized by the G7 rates. The product formation rates of AMY1 wild-type are indicated by the horizontal bars. Asterisk represents values *not* different from wild-type values.

Loss of stacking at subsite −6 in Y105A AMY1 was accompanied by increased DMA of 3.3. This promotion of processivity is plausibly connected with the substantially reduced affinity of Y105A (Table 1). Y105A AMY1, in contrast to wild-type, released no glucose, demonstrating that multiple attacks by the mutant required interaction with more than one aglycone binding subsite (Kramhøft et al., 2005). M53E at subsite −2 (Mori et al., 2002) had very similar kinetics on amylose DP17 to Y105A and also elevated activity on starch, but DMA was 1 and exceptionally low amounts of oligosaccharides were produced (Kramhøft et al., 2005). Thus successful repetitive attacks in M53E occurred less readily than for wild-type AMY1. T212W at subsite +3/+4 had a DMA of 1.4 and formed neither maltotriose nor maltotetraose indicating that productive binding of the reducing end involved subsites +1 and +2 and presumably a region beyond subsite +4. Perhaps T212W AMY1 assumes the S3 binding mode (Fig. 1) that differs from the energetically slightly more favorable S2 (Bak-Jensen et al., 2004), particularly with the interaction area in S3 being changed at subsite +3 and onwards. M298S at subsite +1/+2 decreased DMA to 1.2 and had also impaired contact for short aglycone docking substrate moieties, resulting in less glucose and maltose than wild-type.

In summary, mutations at different subsites significantly affected DMA, whereas the oligosaccharide product profiles only changed markedly for products of

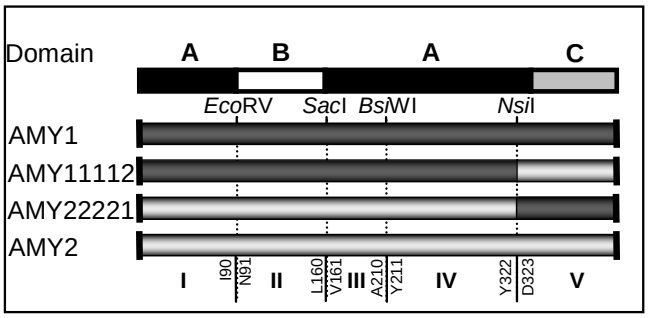

Fig. 5. Schematic of mosaic isozyme chimeras of AMY1 and AMY2. The four restriction sites used for rational construction of the chimeras are shown. The residues at the cross-over points are indicated in AMY2. Adapted with permission from KIM et al. (2003).

DP 1-4. This suggested that enzyme-substrate interactions outside the 10 subsites (subsite −6 through +4; AJANDOUZ et al., 1992) are somehow important since the number of multiple attacks, but not the size of the major products are changed. One may speculate that secondary binding sites on the enzyme surface (see below), or that the conformation of the substrate chain plays an important role in defining the nature of the hydrolysis products. The mechanism of starch degradation may be viewed in analogy to the action of certain cellulases attacking crystalline cellulose fibers in an endo-action followed by subsequent repeated attacks in an apparently exo-type of action to release oligosaccharides. Hence, some common principles may be universally valid amongst glycoside hydrolases to degrade recalcitrant complex substrates.

Specific roles in activity of different parts of AMY1 and AMY2

Using different strategies, some of the distinct differences between AMY1 and AMY2 in substrate kinetics, affinity for starch granules, effect of Ca^{2+} on activity, sensitivity to barley α-amylase/subtilisin inhibitor (BASI), and conformational stability, can be tentatively assigned to specific structural differences between the 80% sequence identical isozymes. Certain AMY2 mimicking variants in the binding site such as AMY1 C95T (subsite −5) and T212Y (subsite +4) resulted in AMY2-like kinetics on the oligosaccharide substrate (SVENSSON et al., 2003). Mutational analysis and crystal structures also enabled identification of groups important for the AMY2 specific sensitivity to BASI (VALLÉE et al., 1998; BØNSAGER et al., 2005). Other properties such as the effect of calcium on activity, differences in enzymatic activity and in affinity for starch granules still elude adequate explanation.

Previously, several AMY1/AMY2 chimeras were produced using homologous recombination in yeast in order to dissect structural features with functional importance, assign specific isozyme properties, and to find a way to circumvent the low heterologous expression of AMY2, the naturally predominant isozyme (JUGE et al., 1993; 1995; RODENBURG et al., 1994; 2000). Using the same approach, different mosaic AMY1/AMY2 chimeras were recently constructed by taking advantage of restriction sites in the two genes (Fig. 5; KIM et al., 2003). Activity of these chimeras on short and long substrates highlighted the importance of individual regions of AMY1 and AMY2 for distinct isozyme enzymatic and stability properties (KIM, T.J., BOZONNET, S., NIELSEN, P.K. & SVENSSON, B., in preparation). For instance a chimera containing AMY2 domain C and all other parts of AMY1 – AMY11112 – improved the apparent affinity for amylose DP440 beyond that of AMY1 (Table 2). In contrast, the chimera with the opposite isozyme distribution, having the domain C from AMY1 – AMY22221 – decreased k_{cat} for the oligosaccharide and amylose DP17, while maintaining the K_m of AMY2, but showed affinity superior to AMY2 only for amylose DP440 (data not shown). This observation suggested that the C-terminal domain plays a prominent role in the activity of the enzyme as suggested earlier (TIBBOT et al., 2002), and that this role may be associated to the presence of the newly discovered oligosaccharide binding site referred to as "a pair of sugar tongs" (see below; ROBERT et al., 2003).

In addition, different isozyme gene shuffling approaches were used to solve the practical problem of poor AMY2 expression in yeast. One such approach involved combinatorial substitution of nucleotide sequence differences between AMY1 and AMY2 by using DOGS (Degenerate Oligonucleotide Gene Shuffling) (GIBBS et al., 2001). The target region His^{14}-Gln^{49} containing 10 amino acid sequence differences between AMY1 and AMY2 was selected based on the increasing expression of AMY1/AMY2 bipartite chimeric genes encoding N-terminal AMY1 parts (JUGE et al., 1993). The resulting best mutant A42P AMY2, selected on starch-plates by expression screening of a variant library, improved the recombinant AMY2 yield in *Saccharomyces cerevisiae* by 2–6 fold, and in *Pichia pastoris* by even 60 fold (FUKUDA et al., 2005) compared to AMY2. Thus, the expression level of A42P AMY2 was comparable to that of AMY1 when both enzymes were produced in *P. pastoris* (JUGE et al., 1996).

Natural and introduced secondary substrate-binding sites

The crystal structure of AMY1 in complex with thiomethyl maltotetraoside revealed a novel binding site in the C-terminal domain (ROBERT et al., 2003) (Fig. 6). Moreover, new binding sites were introduced by genetic fusion between the C-terminus of AMY1 and the starch-binding domain (SBD) of *Aspergillus niger* glucoamylase (JUGE et al., 2002). The binding site in domain C was referred to as "a pair of sugar tongs" since Tyr^{380} moves to capture the oligosaccharide (ROBERT et al.,

Table 2. Enzymatic activities of domain C variants: an AMY1/AMY2 chimera and a "sugar tong" mutant.

AMY1[a]	Cl-pNPG$_7$			Amylose DP440		
	k_{cat} s^{-1}	K_m mM	k_{cat}/K_m s^{-1} mM^{-1}	k_{cat} s^{-1}	K_m mg mL^{-1}	k_{cat}/K_m s^{-1} mg^{-1} mL
AMY1[a]	40	0.76	53	190	0.43	441
AMY2[a]	86	2.1	41	721	1.1	655
AMY 11112[ab]	49	0.84	58	105	0.20	525
AMY1 S378P	59	0.86	69	163	0.20	815

[a] From Kim, T.J., Bozonnet, S., Nielsen, P.K. & Svensson, B. (in preparation).
[b] AMY11112 = AMY1(aa 1-318)/AMY2(aa317-403).

2003). This site was also occupied by maltoheptaose in the inactive mutant D180A of the catalytic nucleophile (Robert et al., 2005). Moreover, binding occurred at a previously discovered surface site (Gibson et al., 1987; Kadziola et al., 1998) where Trp^{278} and Trp^{279} stacked onto two adjacent rings of thiomethyl maltoside (Robert et al., 2003), acarbose, and maltoheptaose (Robert et al., 2005). In contrast to the thiomaltotetraoside, the D180A mutant also bound maltoheptaose and acarbose – and AMY1 wild-type bound the acarbose derived component II – in the substrate binding cleft (Robert et al., 2005).

Although the key residue Tyr^{380} in the "sugar tongs" is conserved in AMY2, no oligosaccharide was bound to domain C in the crystal structure of AMY2 (Kadziola et al., 1998). The K_D for the starch mimic β-cyclodextrin, determined by surface plasmon resonance (SPR), increased from 0.20 mM for AMY1 wild-type to 1.4 mM for the Y380A mutant. AMY1 S378P, an AMY2 mimic, had a K_D of 0.25 mM and superior affinity for amylose DP440 compared to AMY1 (Table 2). As mentioned earlier, the high affinity of certain isozyme chimeras with AMY2 domain C suggested that this domain conferred novel properties which were not observed in wild-type AMY2. In the search for surface sites with a particular role in polysaccharide degradation, DMA on amylose DP440 for Y380A and S378P AMY1 was measured, but found very similar to that of AMY1 wild-type. Structure/function relationships of the sugar tongs is currently investigated by a second series of mutations.

The vast majority of GH-H members are multidomain proteins, including cyclodextrin glycosyltransferase and maltotetraose-forming amylase, which, together with a small group of α-amylases, contain an SBD belonging to family 20 of carbohydrate binding modules (CBM20) (Janecek et al., 2003; http://afmb.cnrs-mrs.fr/CAZY). SBD from *Aspergillus niger* glucoamylase has two β-cyclodextrin binding sites (Sorimachi et al., 1997) and the SBD in cyclodextrin glycosyltransferase binds two maltose molecules (Lawson et al., 1994). In an attempt to confer stronger starch binding to AMY1, a fusion gene encoding AMY1 linked C-terminally to SBD *via* a segment of the polypeptide linker from *A. niger* glucoamylase was constructed. DMA of the AMY1-SBD increased from 1.9 of AMY1 to 3.0 and the fusion produced relatively more malto-oligosaccharides of DP 8–10 than AMY1 (Kramhøft et al., 2005). AMY1-SBD enhanced the rate of release of soluble reducing sugar from barley starch granules up to 15-fold. However, increasing amounts of AMY1-SBD saturated the surface of the starch granules thus loosing the gained efficiency in degradation. This improved activity of AMY1-SBD is comparable to the 100 fold higher activity of intact glucoamylase from *A. niger* compared to a processed form of the enzyme lacking SBD (Svensson et al., 1982). Hence, other parameters, such as the spatial alignment of the SBD and the catalytic module as well as the length, flexibility, and the position of the linker are worth considering for optimizing the mode of action of such fusion proteins.

Degradation of amylopectin and amylose by AMY1

AMY1 hydrolysis of amylopectin followed overall non-Michaelian kinetics, but could be resolved in a slow and a fast reaction, each showing Michaelian behavior, whereas the degradation of the linear amylose DP440 followed a mono-exponential fitting. Though it did not affect the hydrolysis of amylose, β-cyclodextrin, at concentrations matching the affinity of the "sugar tongs", was able to inhibit the fast but not the slow reaction in amylopectin degradation. This inhibition was reduced significantly when "sugar tongs" mutant Y380M was used in the experiment. Thus, this finding suggests that the "sugar tongs" play a distinct role in degradation of amylopectin (Willemoës, M., Bozonnet, S., Kramhøft, B. & Svensson, B., in preparation). Moreover, in the initial stage of amylopectin hydrolysis, about four oligosaccharide molecules, mainly maltoheptaose, were released for each newly generated ethanol-insoluble reducing product. At the more advanced stage of the degradation, however, on average only one oligosaccharide molecule was formed per polysaccharide. This behavior possibly implies that amylopectin A chains are attacked first, followed by attack on B chains after these have become more exposed as a consequence of the degradation of A chains.

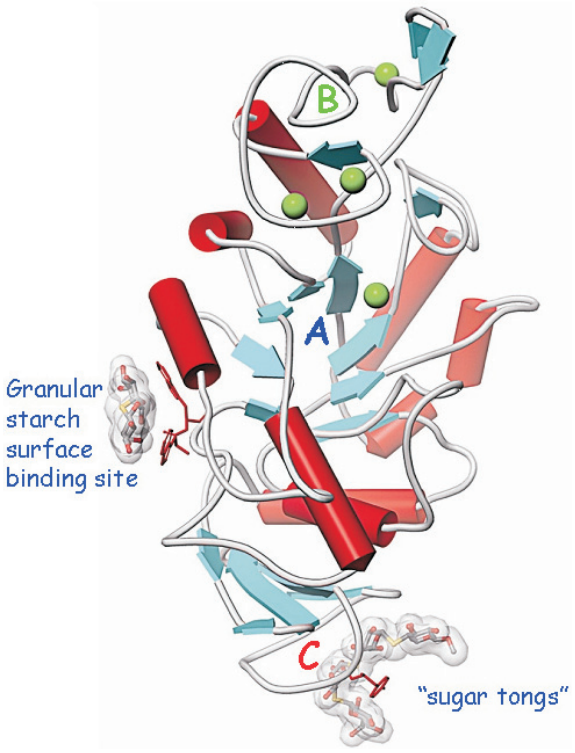

Fig. 6. "Sugar tongs" binding site in AMY1 in complex with methyl trithiomaltotetraoside (thio-DP4; PDB entry 1HT6). At Trp^{278}-Trp^{279} in the catalytic domain, two rings are seen of the tetrasaccharide analogue, whereas the entire molecule is shown to curve around Tyr^{380} in domain C. Adapted with permission from ROBERT et al. (2003).

Proteinaceous α-amylase inhibitors from barley seeds

In nature, α-amylase activity is controlled by a range of proteinaceous inhibitors found mostly in plants (SVENSSON et al., 2004). The structures of complexes between α-amylases and five inhibitor types display different characteristics of the enzyme-inhibitor interaction. These are: (i) porcine pancreatic α-amylase and Tendamistat from *Streptomyces tendae* (WIEGAND et al., 1995); (ii) porcine pancreatic α-amylase and αAI, a lectin-like inhibitor from *Phaseolus vulgaris* (BOMPARD-GILLES et al., 1996); (iii) barley α-amylase 2 (AMY2) and barley α-amylase/subtilisin inhibitor (BASI; Figure 7; VALLÉE et al., 1998); (iv) yellow meal worm α-amylase and a bifunctional inhibitor from *Ragi* (Indian finger millet) (STROBL et al., 1998); and (v) the same enzyme with a small inhibitor from *Amaranth* of the knottin family (PEREIRA et al., 1999). Three of the inhibitors interact directly with the catalytic acids of porcine pancreatic and yellow meal worm α-amylases. In contrast, in AMY2/BASI, an electrostatic network, involving water ligands of a fully hydrated calcium ion at the complex interface, mediates contact between the catalytic acids and side chains of BASI. Cereals are good sources of α-amylase inhibitors (SVENSSON et al., 2004). Mature barley seeds contain an array of

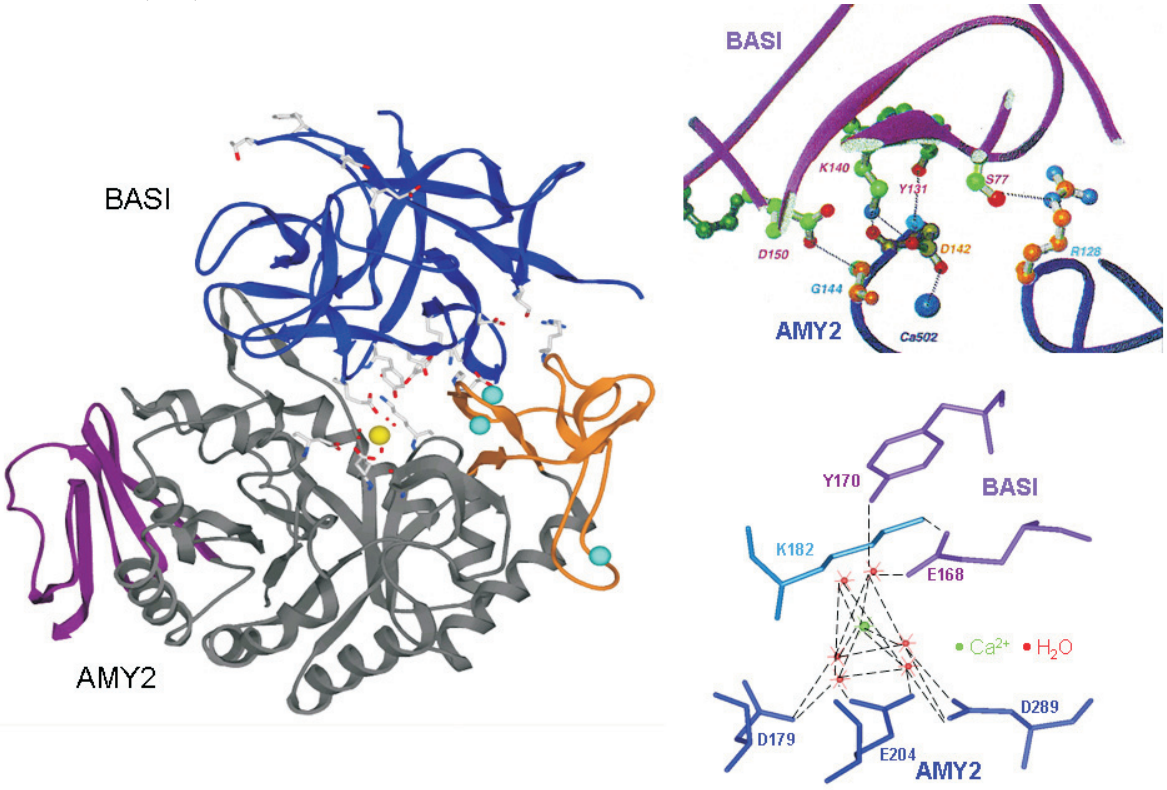

Fig. 7. Three-dimensional structure of AMY2/BASI (VALLÉE et al., 1998; PDB entry 1AVA) and close up focusing on the domain B interaction and the interaction involving the fully hydrated calcium (Ca503) on the protein interface. Adapted with permission from VALLÉE et al. (1998).

Table 3. SPR derived binding parameters and K_i for AMY2 and BASI mutants.

BASI[a]	$k_{on} \times 10^5$ (M^{-1} s^{-1})	$k_{off} \times 10^{-4}$ (s^{-1})	K_D (nM)	K_i (nM)
Wild-type	1.34 (±0.46)	1.6 (±0.2)	1.1 (±0.3)	0.09
S77A	0.86 (±0.46)	3.3 (±0.1)	3.9 (±0.5)	0.35
K140N	0.51 (±0.13)	26.0 (±2.8)	50.0 (±2.8)	21.0
E168Q	1.66 (±0.31)	13.6 (±1.7)	8.2 (±0.4)	2.5

[a] Produced using the intein-CBD-tag system (Bønsager et al., 2005).
The rate constants represent mean of determinations using five BASI concentrations (61–245 nM). Standard deviations are shown in parentheses. Measurements were performed at 25 °C in 10 mM Hepes, pH 8.0, 5 mM $CaCl_2$, 0.005% surfactant P20.

inhibitors acting either on target enzymes from potential pests and pathogens or on the endogenous AMY2. Remarkably, BASI only inhibits AMY2, and not AMY1 (exhibiting 80% sequence identity to AMY2). In addition, the small protein disulfide reductase thioredoxin h (Trx-h) in barley acts on several enzymes and proteins (Maeda et al., 2004) and may thus influence the level of enzyme activity either directly or indirectly by regulating the activity of the inhibitors.

Earlier mutational analysis identified certain AMY2 residues critical for binding BASI and indicated that a few substitutions might render AMY1 sensitive to BASI (Rodenburg et al., 2000). Recent heterologous expression of BASI (Bønsager et al., 2003) allowed for studies of structure/function relationships employing mutational analysis. Thus, while the mutants R128Q and D142N in the target enzyme increased K_i from 0.22 nM to 18 and 28 nM, respectively (Rodenburg et al., 2000), BASI mutants S77A and K140N, interacting with Arg^{128} and Asp^{142}, gave K_i of 0.35 nM and 21 nM, respectively (Bønsager et al., 2005). SPR analysis of AMY2 binding by these and other BASI mutants indicates a generally large effect on k_{off} while k_{on} showed little change (Nielsen et al., 2003; Bønsager et al., 2005) (Table 3). Mutations of BASI residues at the large interface of the protein complex (Vallée et al., 1998) allowed different roles to be ascribed to these residues (Fig. 7). Thus, E168Q implicated Glu^{168} to be important for the stability of the AMY2/BASI complex (Table 3). Increasing concentration of Ca^{2+} improved affinity of wild-type BASI to AMY2, in contrast to E168Q, which resulted in significantly diminished role of Ca^{2+} on the affinity of BASI. These results suggest that the interface Ca^{2+} (Ca503; Fig. 7) is a part of the electrostatic complementarity between AMY2 and BASI. In another area of BASI in contact with AMY2 domain B, which carries isozyme specificity determinants, single mutants also decreased the affinity by 25–120 fold due to increased k_{off} (Bønsager et al., 2005). Combined insight emerging from recent results of BASI mutants with an earlier study of AMY2 mutants interacting with the same side chains in BASI (Rodenburg et al., 2000) – in particular with regard to increased sensitivity to electrostatic screening – emphasized the pivotal role of salt bridges in the affinity of BASI to AMY2 (Bønsager et al., 2005). Another conclusion from the above study was that a few hot spots of interactions, clustered at the center of AMY2/BASI and mainly being charged residues involved in multiple interactions, govern the affinity of BASI to AMY2, with the rest of the contact residues observed in the three-dimensional structure making limited contribution. For instance, mutants showed that the BASI peripheral residues Ser^{77} and Asp^{156} had a significant, albeit limited effect on affinity as compared to Asp^{150} or Glu^{168}, which resulted in a precipitous reduction in the inhibitory potency of BASI (Bønsager et al., 2005).

In addition to BASI, extracts of mature barley seeds, similarly to other cereals (Svensson et al., 2004), contain inhibitors directed towards porcine pancreatic α-amylase and yellow meal worm α-amylase. RP-HPLC on a C4 column of a barley seed extract resolved such activities, possessed by two different CM-proteins, the barley monomeric α-amylase inhibitor (BMAI) and the barley dimeric α-amylase inhibitor (BDAI). CM-proteins belong to a highly diverse and large protein family of which several members with different functionalities are identified in multiple forms in the barley seed proteome (Østergaard et al., 2004). Non-glycosylated and glycosylated BMAI forms were purified and bound yellow meal worm α-amylase at pH 6.5 with K_D of 0.1 and 0.3 μM, respectively, as determined by SPR analysis after biotinylation and inhibitor coupling to a streptavidin chip. Thirty-fold stronger binding was observed at pH 5.0. Similarly, K_D was determined to 0.04 μM for BDAI binding to the biotinylated porcine pancreatic α-amylase-streptavidin chip at pH 6.5 (Nielsen, P.K., Finnie, C., Østergaard, O. & Svensson, B., in preparation).

The different α-amylase inhibitors from barley are targets of Trx-h presently identified in two isoforms in mature seeds (Maeda et al., 2003; 2004). Trx-h specifically acted primarily on one of the two disulfide bonds in BASI and on one disulfide in BMAI and another in BDAI both having five conserved disulfide bonds characteristic to CM-proteins (Maeda et al., 2005). Trx-h has a range of target proteins, including the limit dextrinase inhibitor (MacGregor, 2004), another CM-protein that acts on the limit dextrinase of GH13, which specifically hydrolyses α-1,6 linkages in starch. It is an open question how these various inhibitors and Trx-h interact to contribute to the level and specificity of the starch-degrading activity in germinating seeds or act in concert for seed defense against pathogens and pests.

Conclusion and perspectives

Increasing knowledge on AMY1 and AMY2 and interactions with substrates and inhibitors illustrate the complexity of enzymatic degradation of polymeric substrates and the underlying mechanisms implemented and fine-tuned with structural subtleness. In particular, novel data on sugar recognition at a certain distance from the active site advance the understanding of the biological roles of these enzymes. Isozyme chimeras, family gene shuffling, and other directed evolution approaches are excellent tools for gaining insight into structure/function relationships paradigm for GH13 members. Although proteomes present only snapshots to be compiled for temporal and spatial variation of the studied organism, information on turn-over of multiple forms of AMY2 in germinating seeds will inspire new thinking (Bak-Jensen, K.S., Laugesen, S., Østergaard, O., Finnie, C., Roepstorff, P. & Svensson, B., in preparation).

Only some GH-H members, including almost all α-amylases, require calcium ions for stability and activity. Besides a highly conserved calcium ion, α-amylase structures contain other calcium ions at varying positions. Thorough analysis of the calcium requirement and effects of introducing or removing calcium through protein engineering have barely been addressed. Future developments should take advantage of coupling classical biochemical tools and rational mutation with *in vitro* evolution approaches to surmount the challenges inherent with this type of studies. A special asset in rational engineering of amylolytic enzyme is the knowledge on sugar ligand conformation and binding energies obtained from structures of crystallographic or modeled complexes evaluated by molecular recognition approaches.

The modular architecture of amylolytic enzymes motivates creation of fusion proteins with advantageous combinations of functionalities, e.g. ability to bind insoluble substrates, or manipulation of activity for various substrate categories, e.g. branched dextrins. This approach entails considering substrate-binding sites outside of the active site region, or the extension of the active site by aid of auxiliary modules, either to enhance or to modify substrate preference and mode of action of target enzymes. Structural insight, and hence the understanding of the concerted action of catalytic and other remote substrate subsites is highly limited. Questions remain on the mechanism of action and role of such sites in enzymatic conversions and utilization of sugars, and how individual domains interact during catalysis. This has special relevance for action on high-molecular mass substrates. Finally, participation of α-amylases in interaction networks containing protein inhibitors and regulatory proteins, such as thioredoxin, places these enzymes into a complicated biological context of which the description is at its infancy.

Acknowledgements

The expert technical assistance of Sidsel Ehlers and Janni Carina Larsen is gratefully acknowledged. The work has been supported by the EU-projects AGADE (BIO4-CT98-0022), GEMINI (QLK-2000-000811), and CEGLYC (QLK3-CT-2001-00149) and the Danish Natural Science Research Council (grants 21-03-0071; 21-03-0338).

References

Ajandouz, E.H., Abe, J., Svensson, B. & Marchis-Mouren, G. 1992. Biochim. Biophys. Acta **1159:** 193–202.

André, G. & Tran, V. 1999. pp. 165–175. In: Gilbert, H.J, Davies, G.J., Henrissat, B. & Svensson, B. (eds) Recent Advances in Carbohydrate Bioengineering, Royal Society of Chemistry, Cambridge.

Bak-Jensen, K.S., André, G., Gottschalk, T.E., Paës, G, Tran, V. & Svensson, B. 2004. J. Biol. Chem. **279:** 10093–10102.

Bompard-Gilles, C., Rousseau, P., Rougé, P. & Payan, F. 1996. Structure **4:** 1441–1452.

Bønsager, B.C., Nielsen, P.K., Abou Hachem, M., Fukuda, K., Prætorius-Ibba, M., & Svensson, B. 2005. J. Biol. Chem. **280:** 14855–14864.

Bønsager, B.C., Prætorius-Ibba, M., Nielsen, P.K. & Svensson, B. 2003. Protein Express. Purif. **30:** 185–193.

Brzozowski, A.M., Lawson, D.M., Turkenberg, J.P., Bisgård-Frantzen, H., Svendsen, A., Borchert, T.V., Dauter, Z., Wilson, K.S. & Davies, G.J. 2000. Biochemistry **39:** 9099–9107.

Coutinho, P.M. & Henrissat, B. 1999. pp. 3–12. In: Gilbert, H.J, Davies, G.J., Henrissat, B. & Svensson, B. (eds) Recent Advances in Carbohydrate Bioengineering, Royal Society of Chemistry, Cambridge.

Fukuda, K., Jensen, M.H., Haser, R., Aghajari, N. & Svensson, B. 2005. Protein Eng. Des. Sel. **18:** 515–526.

Giardina, T., Gunning, A.P., Juge, N., Faulds, C.B., Furniss, C.S.M., Svensson, B., Morris, V.J. & Williamson, G. 2001. J. Mol. Biol. **313:** 1149–1159.

Gibbs, M.D., Nevalainen, K.M. & Bergquist, P.L. 2001. Gene **271:** 13–20.

Gibson, R.M. & Svensson, B. 1987. Carlsberg Res. Commun. **52:** 373–379.

Gottschalk, T.E., Tull, D., Aghajari, N., Haser, R. & Svensson, B. 2001. Biochemistry **40:** 12844–12854.

Janecek, S., Svensson B. & MacGregor, E.A. 2003. Eur. J. Biochem. **270:** 635–645.

Juge, N., Andersen, J.S., Tull, D., Roepstorff, P. & Svensson, B. 1996. Protein Express. Purif. **8:** 204–214.

Juge, N., Le Gal-Coëffet, M.F., Furniss, C.S.M., Gunning, P., Kramhøft, B., Morris, V.J., Svensson, B. & Williamson, G. 2002. Biologia, Bratislava **57 (Suppl. 11):** 239–245.

Juge, N., Rodenburg, K.W., Guo, X.J., Chaix, J.C. & Svensson, B. 1995. FEBS Lett. **263:** 299–303.

Juge N., Søgaard, M., Chaix, J.C., Martin-Eauclaire, M.F., Svensson, B., Marchis-Mouren, G. & Guo, X.J. 1993. Gene **130:** 159–166.

Kadziola, A., Søgaard, M., Svensson, B. & Haser, R. 1998. J. Mol. Biol. **279:** 205–217.

Kim, T.J., Bozonnet, S., Nielsen, P.K. & Svensson B. 2003. pp. 9–17. In: Carbohydrate: Enzymes and Food Functionality (Proceedings of Agricultural Biotechnology Symposium), Center for New Bio-Materials in Agriculture, Seoul National University.

Kramhøft, B., Bak-Jensen, K.S., Mori, H., Juge, N., Nøhr, J. & Svensson, B. 2005. Biochemistry **44:** 1824–1832.

Lawson, C.L., Van Montfort, R., Strokopytov, B., Rozeboom, H.J., Kalk, K.H., De Vries, G.E., Penninga, D.,

Dijkhuizen, L. & Dijkstra, B.W. 1994. J. Mol. Biol. **236:** 590–600.
MacGregor, E.A. 2004. Biochim. Biophys. Acta **1696:** 165–170.
MacGregor, E.A., Janecek, S. & Svensson, B. 2001. Biochim. Biophys. Acta **1546:** 1–20.
MacGregor, E.A., Jespersen, H.M. & Svensson, B. 1996. FEBS Lett. **378:** 263–266.
Maeda, K., Finnie, C., Østergaard, O. & Svensson, B. 2003. Eur. J. Biochem. **270:** 2633–2643.
Maeda, K., Finnie, C. & Svensson, B. 2004. Biochem. J. **378:** 497–507.
Maeda, K., Finnie, C. & Svensson, B. 2005. Proteomics **5:** 1634–1644.
Matsui, I. & Svensson, B. 1997. J. Biol. Chem. **272:** 22456–22463.
Mori, H., Bak-Jensen, K.S., Gottschalk, T.E., Motawia, M.S., Damager, I., Møller, B.L. & Svensson, B. 2001. Eur. J. Biochem. **268:** 6545–6558.
Mori, H., Bak-Jensen, K.S. & Svensson, B. 2002. Eur. J. Biochem. **269:** 5377–5390.
Nielsen, P. K., Bønsager, B. C., Berland, C. R. Sigurskjold, B. W. & Svensson, B. 2003. Biochemistry **42:** 1478–1487.
Østergaard, O., Finnie, C., Laugesen, S., Roepstorff, P. & Svensson, B. 2004. Proteomics **4:** 2437–2447.
Pereira, P.J.B., Lozanov, V., Patthy, A., Huber, R., Bode, W. & Strobl, S. 1999. Structure **7:** 1079–1088.
Przylas, I., Terada, Y., Fujii, K., Takaha, T., Saenger, W. & Sträter, N. 2000. Eur. J. Biochem. **267:** 6903–6913.
Robert, X., Gottschalk, T.E., Haser, R., Svensson, B. & Aghajari, N. 2002a. Acta Cryst. **D58:** 686–686.
Robert, X., Haser, R., Gottschalk, T.E., Ratajczek, F., Driguez, H., Svensson, B. & Aghajari, N. 2003. Structure **11:** 973–984.
Robert, X., Haser, R., Mori, H., Svensson, B. & Aghajari, N. 2005. J. Biol. Chem. **280:** 32968–32978.
Robert, X., Haser, R., Svensson, B. & Aghajari, N. 2002b. Biologia, Bratislava **57 (Suppl. 11):** 59–70.
Robyt, J.F. & French, D. 1967. Arch. Biophys. Biochem. **122:** 8–16.
Rodenburg, K.W., Juge, N., Guo, X.J., Søgaard, M., Chaix, J.C. & Svensson, B. 1994. Eur. J. Biochem. **221:** 277–284.
Rodenburg, K.W., Vallée, F., Juge, N., Aghajari, N., Guo, X.J., Haser, R. & Svensson, B. 2000. Eur. J. Biochem. **267:** 1019–1029.
Sorimachi, K., Le Gal-Coëffet, M.F., Williamson, G., Archer, D.B. & Williamson, M.P. 1997. Structure **5:** 647–661.
Strobl, S., Maskos, K., Wiegand, G., Huber, R., Gomis-Rüth, F.X. & Glockshuber, R. 1998. Structure **6:** 911–921.
Svensson B., Fukuda, K. Nielsen, P.K & Bønsager, B.C. 2004. Biochim. Biophys. Acta. **1696**: 145–156.
Svensson B., Mori, H., Bak-Jensen, K.S. & Jensen, M.T. 2003. J. Appl. Glycosci. **50:** 143–145.
Svensson, B., Pedersen, T.G., Svendsen, I., Sakai, T. & Ottesen, M. 1982. Carlsberg Res. Commun. **47:** 55–69.
Søgaard, M., Kadziola, A., Haser, R. & Svensson, B. 1993. J. Biol. Chem. **268:** 22480–22484.
Tibbot, K.B., Wong, D.W.S. & Robertson, G.H. 2002. Biologia, Bratislava **57 (Suppl. 11):** 229–238.
Vallée, F., Kadziola, A., Bourne, Y., Juy, M., Rodenburg, K.W., Svensson, B. & Haser, R. 1998. Structure **6:** 649–659.
Wiegand, G., Epp, O. & Huber, R. 1995. J. Mol. Biol. **247:** 99–110.

Received February 3, 2005
Accepted April 21, 2005